2005 American Control Conference
June 8-10, 2005. Portland, OR, USA

Data-driven Kalman Filters for Non-uniformly Sampled Multirate Systems with Application to Fault Diagnosis

Weihua Li and Sirish Shah

Abstract— **This paper first develops data-driven Kalman filters for non-uniformly sampled multirate systems. Then a novel methodology of fault detection and isolation for such systems is proposed. The proposed scheme is applied to a pilot scale experimental plant, where a successful case study on FDI is conducted.**

I. INTRODUCTION

Originally developed in the 1960s [1], Kalman filters have demonstrated their power in state estimation, system identification, adaptive control, signal processing [2] and found widely varying industrial applications [3]. Many variants of Kalman filtering algorithms have been proposed [4]. However, most of them are for single rate discrete-time (DT) systems.

In many industrial processes, variables are sampled at more than one rate, i.e. *multiple rates*. Take a polymer reactor as an example, where the manipulated variables can be adjusted at relatively fast rates [5], while the measurements of quality variables, e.g. the composition and density, are typically obtained after several minutes of laboratory analysis. Furthermore, the sampling is called *non-uniform*, if the sampling intervals for each variable are *non-equally* spaced.

We have developed Kalman filters for a non-uniformly sampled multirate (NUSM) system [6], assuming that the model, referred to as *lifted model*, and the covariances of relevant noise and disturbance are known *a priori*. Since such an assumption may lose its validity in practical situations, we are motivated to develop data-driven Kalman filters by proposing a subspace method of identification (SMI) for the afore-mentioned model and covariances.

Since the late 1980s, the SMI has been an active research area and successfully applied to multivariate DT systems with a single rate [7], [8], [9]. In comparison with the traditional prediction errors methods of identification [10], the SMI has better numerical properties for systems with high dimensionality. A literature overview and comparison on several popular SMIs have been given in [11].

Recently, SMIs for multirate systems have been reported. However, they are developed either only for uniformly sampled systems [12] or for NUSM systems with a special purpose, e.g. identification of residual models for fault detection and isolation (FDI) [13]. This paper focuses on the development of data-driven Kalman filters for NUSM systems, including a SMI algorithm to estimate the state space model, e.g. $\{\underline{\mathbf{A}}, \underline{\mathbf{B}}, \underline{\mathbf{C}}, \underline{\mathbf{D}}\}$, as well as the relevant noise covariances of the NUSM systems. Another main component of this paper is the development of a novel Kalman filter-based approach towards FDI for NUSM systems.

W. Li and S.L. Shah are with the Department of Chemical and Materials Engineering, University of Alberta, Edmonton, Alberta, T6G 2G6, Canada. {weihua,sirish.shah}@ualberta.ca

II. PROBLEM FORMULATION

Consider a continuous-time (CT) state space system:

$$\begin{aligned} \dot{\mathbf{x}}(t) &= \mathbf{A}\mathbf{x}(t) + \mathbf{B}\tilde{\mathbf{u}}(t) + \boldsymbol{\phi}(t) \\ \tilde{\mathbf{y}}(t) &= \mathbf{C}\mathbf{x}(t) + \mathbf{D}\tilde{\mathbf{u}}(t) \end{aligned} \quad (1)$$

where (i) $\tilde{\mathbf{u}}(t) \in \Re^l$ and $\tilde{\mathbf{y}}(t) \in \Re^m$ are *noise-free* inputs and outputs, respectively; (ii) $\mathbf{x}(t) \in \Re^n$ is the state; (iii) $\boldsymbol{\phi}(t)$ is the disturbance assumed to be a Gaussian distributed white noise vector with covariance $\mathbf{R}_\phi$, i.e. $\boldsymbol{\phi}(t) \sim \aleph(\mathbf{0}, \mathbf{R}_\phi)$; and (iv) $\mathbf{A}$, $\mathbf{B}$, $\mathbf{C}$ and $\mathbf{D}$ are unknown system matrices with compatible dimensions. Note that in the sequel throughout the paper, we use the notation, $\aleph(\mathbf{0}, \mathbf{R})$, to stand for a Gaussian distributed white noise vector with covariance $\mathbf{R}$. It is further assumed that (i) the pair $(\mathbf{A}, \mathbf{C})$ is observable, (ii) the pair $(\mathbf{A}, \mathbf{B}\mathbf{R}_\phi^{1/2})$ is controllable, and (iii) the stochastic part of $\mathbf{A}$ is asymptotically stable.

A. The lifted model for a NUSM system

The non-uniformly multirate sampling approach [14] is employed to collect measurements from Eqn. 1. For a given *frame period*, T, over the k^{th} frame period $[kT, kT+T)$, the inputs and outputs are sampled as follows.

- An input variable is sampled g times at time instants: $\{kT+t_1, kT+t_2, kT+t_3, \cdots, kT+t_g\}$, where $0 = t_1 < t_2 < \cdots < t_g < T$.
- An output variable is sampled p times. Moreover, within the time interval $[kT+t_i, kT+t_{i+1})$, for $i = [1, ..., g]$, n_i (≥ 0) samples of the output variable are taken at time instants: $\{kT+t_i^1, kT+t_i^2, \cdots, kT+t_i^{n_i}\}$, where $t_i \leq t_i^1 < t_i^2 \cdots < t_i^{n_i} < t_{i+1}$ and $t_{g+1} = T$. Note that $p = n_1 + n_2 + \cdots + n_g$ can be larger/less than, or equal to g.

The sampling is repeated over the next frame period.

In the most general case, among the $m+l$ inputs and outputs, each variable is sampled differently from the others. However, for simplicity of mathematical manipulation and without loss of generality it is assumed that (i) the l inputs, $\tilde{\mathbf{u}}(t)$, and the disturbances are sampled at one rate; and (ii) the m outputs, $\tilde{\mathbf{y}}(t)$, are sampled at the other rate.

0-7803-9098-9/05/$25.00 ©2005 AACC

Accordingly, the lifted vectors for inputs and outputs are constructed as follows, respectively,

$$\underline{\tilde{\mathbf{u}}}(k) = \begin{bmatrix} \tilde{\mathbf{u}}(kT+t_1) \\ \vdots \\ \tilde{\mathbf{u}}(kT+t_g) \end{bmatrix}, \ \underline{\tilde{\mathbf{y}}}(k) \equiv \begin{bmatrix} \tilde{\mathbf{y}}(kT+t_1^1) \\ \vdots \\ \tilde{\mathbf{y}}(kT+t_1^{n_1}) \\ \vdots \\ \tilde{\mathbf{y}}(kT+t_g^1) \\ \vdots \\ \tilde{\mathbf{y}}(kT+t_g^{n_g}) \end{bmatrix}.$$

In addition, the lifted vector for the disturbance, $\underline{\boldsymbol{\phi}}(k)$, is structurally identical to $\underline{\tilde{\mathbf{u}}}(k)$.

At the time instant $kT+t_i^j$, for $j=[1,n_i]$, the sampled outputs are

$$\mathbf{y}(kT+t_i^j) = \tilde{\mathbf{y}}(kT+t_i^j) + \mathbf{o}(kT+t_i^j) \tag{2}$$

where $\mathbf{o}(\ ) \sim \aleph(\mathbf{0}, \mathbf{R}_o)$ is the measurement error and independent of the initial state, $\mathbf{x}(0)$. However, at instant $kT+t_i$ for $i=[1,g]$, assume that $\tilde{\mathbf{u}}(kT+t_i)$ be available, i.e. $\mathbf{u}(kT+t_i) = \tilde{\mathbf{u}}(kT+t_i)$, because in a closed-loop system they are outputs of controllers and can be known.

It follows from Eqn. 2 that $\underline{\mathbf{y}}(k) = \underline{\tilde{\mathbf{y}}}(k) + \underline{\mathbf{o}}(k)$, where $\underline{\mathbf{y}}(k)$ and $\underline{\mathbf{o}}(k)$ have the identical structure to $\underline{\tilde{\mathbf{y}}}(k)$. Besides, $\underline{\mathbf{o}}(k) \sim \aleph(\mathbf{0}, \underline{\mathbf{R}}_o)$ with $\underline{\mathbf{R}}_o = \mathbf{I}_p \otimes \mathbf{R}_o$, where $\otimes$ is the Kronecker tensor product and $\mathbf{I}_l$ denotes an $l \times l$ identity matrix. In the sequel, any $\kappa \times \kappa$ identity matrix is denoted by $\mathbf{I}_\kappa$. The lifted model of Eqn. 1 can be derived as follows [14]:

$$\begin{aligned} \mathbf{x}(k+1) &= \underline{\mathbf{A}}\ \mathbf{x}(k) + \underline{\mathbf{B}}\ \underline{\mathbf{u}}(k) + \underline{\mathbf{W}}\ \underline{\boldsymbol{\phi}}(k) \\ \underline{\mathbf{y}}(k) &= \underline{\mathbf{C}}\ \mathbf{x}(k) + \underline{\mathbf{D}}\ \underline{\mathbf{u}}(k) + \underline{\mathbf{J}}\ \underline{\boldsymbol{\phi}}(k) + \underline{\mathbf{o}}(k) \end{aligned} \tag{3}$$

where (i) $\underline{\mathbf{A}}$, $\underline{\mathbf{B}}$, $\underline{\mathbf{C}}$, $\underline{\mathbf{D}}$, $\underline{\mathbf{J}}$, and $\underline{\mathbf{W}}$ are functions of $\mathbf{A}$, $\mathbf{B}$, $\mathbf{C}$, $\mathbf{D}$, t_i, and $t_i^{n_i}$, $\forall\ i=1,\cdots,g$; (ii) $\underline{\boldsymbol{\phi}}(k) \sim \aleph(\mathbf{0}, \underline{\mathbf{R}}_\phi)$ with $\underline{\mathbf{R}}_\phi = \mathbf{I}_n \otimes \mathbf{R}_\phi$. It is assumed that the frame period T is non-pathological relative to matrix $\mathbf{A}$. As a consequence, Eqn. 3 preserves the causality, controllability and observability of Eqn. 1 [14]. Denote $\underline{\boldsymbol{\omega}}(k) \equiv \underline{\mathbf{W}}\ \underline{\boldsymbol{\phi}}(k)$ and $\underline{\boldsymbol{\varepsilon}}(k) \equiv \underline{\mathbf{J}}\ \underline{\boldsymbol{\phi}}(k) + \underline{\mathbf{o}}(k)$, which have the following auto/cross-covariances:

$$\underline{\mathbf{R}}_\omega = \underline{\mathbf{W}}\ \underline{\mathbf{R}}_\phi \underline{\mathbf{W}}', \underline{\mathbf{R}}_\varepsilon = \underline{\mathbf{J}}\ \underline{\mathbf{R}}_\phi \underline{\mathbf{J}}' + \underline{\mathbf{R}}_o, \underline{\mathbf{R}}_{\omega,\varepsilon} = \underline{\mathbf{W}}\ \underline{\mathbf{R}}_\phi \underline{\mathbf{J}}'.$$

Consequently, we rewrite Eqn. 3 as

$$\begin{aligned} \mathbf{x}(k+1) &= \underline{\mathbf{A}}\ \mathbf{x}(k) + \underline{\mathbf{B}}\ \underline{\mathbf{u}}(k) + \underline{\boldsymbol{\omega}}(k) \\ \underline{\mathbf{y}}(k) &= \underline{\mathbf{C}}\ \mathbf{x}(k) + \underline{\mathbf{D}}\ \underline{\mathbf{u}}(k) + \underline{\boldsymbol{\varepsilon}}(k) \end{aligned} \tag{4}$$

Eqn. 4 is the lifted model of a NUSM system.

B. Problem statement

Kalman filters for the lifted system of Eqn. 4 are [6]:

$$\begin{aligned} \hat{\mathbf{x}}(k+1|k) &= \underline{\mathbf{A}}\ \hat{\mathbf{x}}(k|k-1) + \underline{\mathbf{B}}\ \underline{\mathbf{u}}(k) + \\ &\quad \underline{\mathbf{L}}(k)\left[\underline{\mathbf{y}}(k) - \underline{\mathbf{C}}\ \hat{\mathbf{x}}(k|k-1) - \underline{\mathbf{D}}\ \underline{\mathbf{u}}(k)\right] \end{aligned} \tag{5}$$

where, $\hat{\mathbf{x}}(i+1|i)$ is the unbiased estimate of $\mathbf{x}(i+1)$ from $\{\underline{\mathbf{u}}(1), \underline{\mathbf{y}}(1), \cdots, \underline{\mathbf{u}}(i), \underline{\mathbf{y}}(i)\}$ for $i=k-1$ or $i=k$ with initial value, $\hat{\mathbf{x}}(0|-1) = \mathbf{E}[\mathbf{x}(0)]$. Note that $\mathbf{E}(\ )$ represents the mean of the argument. In addition,

$$\underline{\mathbf{L}}(k) = \left(\underline{\mathbf{A}}\ \underline{\mathbf{M}}(k)\underline{\mathbf{C}}' + \underline{\mathbf{R}}_{\omega,\varepsilon}\right)\underline{\mathbf{G}}^{-1}(k)$$

is the Kalman gain, where

$$\begin{aligned} \underline{\mathbf{G}}(k) &= \underline{\mathbf{C}}\ \underline{\mathbf{M}}(k)\underline{\mathbf{C}}' + \underline{\mathbf{R}}_\varepsilon \\ \underline{\mathbf{M}}(k+1) &= \underline{\mathbf{A}}\ \underline{\mathbf{M}}(k)\underline{\mathbf{A}}' + \underline{\mathbf{R}}_\omega - \\ &\quad \left[\underline{\mathbf{A}}\ \underline{\mathbf{M}}(k)\underline{\mathbf{C}}' + \underline{\mathbf{R}}_{\omega,\varepsilon}\right]\underline{\mathbf{G}}^{-1}(k) \bullet \\ &\quad \left[\underline{\mathbf{A}}\ \underline{\mathbf{M}}(k)\underline{\mathbf{C}}' + \underline{\mathbf{R}}_{\omega,\varepsilon}\right]' \end{aligned}$$

with $(\ )'$ standing for the transpose of the argument.

This paper considers the following problems:

- Given data: $\{\underline{\mathbf{u}}(1), \underline{\mathbf{y}}(1), \cdots, \underline{\mathbf{u}}(N), \underline{\mathbf{y}}(N)\}$, as $N \to \infty$, develop a SMI to estimate the system matrices, $\underline{\mathbf{A}}$, $\underline{\mathbf{B}}$, $\underline{\mathbf{C}}$, and $\underline{\mathbf{D}}$; the covariances, $\underline{\mathbf{R}}_\epsilon$, $\underline{\mathbf{R}}_\omega$, $\underline{\mathbf{R}}_{\omega,\varepsilon}$;
- Construct the Kalman filters of Eqn. 5, and further investigate a Kalman filter-based FDI methodology for NUSM systems.

III. The subspace identification algorithms

In this section, by extending the N4SID algorithms [15] from single rate DT systems to NUSM systems, we propose SMI for the system described by Eqn. 4. The derivation of the identification algorithm is similar to that in the N4SID. Therefore, only the main results are provided.

A. The stacked equations

For any positive integer j, we define a reversed extended controllability matrix, $\underline{\Delta}_j \equiv [\underline{\mathbf{A}}^{j-1}\underline{\mathbf{B}}\ \ \underline{\mathbf{A}}^{j-2}\underline{\mathbf{B}}\ \ \cdots\ \ \underline{\mathbf{A}}\ \ \underline{\mathbf{B}}\ \ \underline{\mathbf{B}}]$; and a stacked vector,

$$\underline{\boldsymbol{\xi}}_j(k) = \left[\ \underline{\boldsymbol{\xi}}'(k)\ \ \cdots\ \ \underline{\boldsymbol{\xi}}'(k+j-1)\ \right]',$$

where $\underline{\boldsymbol{\xi}}(k)$ can be $\underline{\mathbf{u}}(k)$, $\underline{\mathbf{y}}(k)$, $\underline{\boldsymbol{\omega}}(k)$, or $\underline{\boldsymbol{\varepsilon}}(k)$. From time instants k up to $k+j$, applying repeated recursions to Eqn. 4 yields

$$\begin{aligned} \mathbf{x}(k+j) &= \underline{\mathbf{A}}^j\mathbf{x}(k) + \underline{\Delta}_j\underline{\mathbf{u}}_j(k) + \underline{\Delta}_j^s\underline{\boldsymbol{\omega}}_j(k) \\ \underline{\mathbf{y}}(k+j) &= \underline{\mathbf{C}}[\underline{\mathbf{A}}^j\mathbf{x}(k) + \underline{\Delta}_j\underline{\mathbf{u}}_j(k) + \underline{\Delta}_j^s\underline{\boldsymbol{\omega}}_j(k)] \\ &\quad + \underline{\mathbf{D}}\ \underline{\mathbf{u}}(k+j) + \underline{\boldsymbol{\varepsilon}}(k+j) \end{aligned} \tag{6}$$

where $\underline{\Delta}_j^s = \underline{\Delta}_j|_{\underline{\mathbf{B}}=\mathbf{I}_n}$ and we define $\underline{\Delta}_j \equiv \mathbf{0}$ if $j=0$.

Define an extended observability matrix ($i > n$),

$$\underline{\boldsymbol{\Gamma}}_i \equiv [\underline{\mathbf{C}}'\ \underline{\mathbf{A}}'\underline{\mathbf{C}}'\ \ \cdots \left(\underline{\mathbf{A}}^{i-1}\right)'\underline{\mathbf{C}}']' \in \Re^{imp\times n}$$

and a lower block triangular Toeplitz matrix,

$$\underline{\mathbf{H}}_i \equiv \left[\begin{array}{c|c} \underline{\mathbf{D}} & \mathbf{0} \\ \hline \underline{\boldsymbol{\Gamma}}_{i-1}\underline{\mathbf{B}} & \underline{\mathbf{H}}_{i-1} \end{array}\right] \in \Re^{imp\times igl}$$

with $\underline{\mathbf{H}}_0 = \underline{\mathbf{D}}$. We emphasize that $\underline{\boldsymbol{\Gamma}}_i$ has rank n because the pair $(\underline{\mathbf{C}}, \underline{\mathbf{A}})$ is observable. Stacking Eqn. 6 from $j=0$ until $j=i-1$ provides

$$\underline{\mathbf{y}}_i(k) = \underline{\boldsymbol{\Gamma}}_i\mathbf{x}(k) + \underline{\mathbf{H}}_i\underline{\mathbf{u}}_i(k) + \underline{\boldsymbol{\pi}}_i(k) \tag{7}$$

where $\underline{\boldsymbol{\pi}}_i(k) = \underline{\mathbf{H}}_i^s\underline{\boldsymbol{\omega}}_i(k) + \underline{\boldsymbol{\varepsilon}}_i(k)$, and $\underline{\mathbf{H}}_i^s = \underline{\mathbf{H}}_i|_{\underline{\mathbf{B}}=\mathbf{I}_n, \underline{\mathbf{D}}=\mathbf{0}}$.

Define a block Hankel matrix for the inputs,

$$\underline{\mathbf{U}}_{0,i-1} = \begin{bmatrix} \underline{\mathbf{u}}(0) & \underline{\mathbf{u}}(1) & \cdots & \underline{\mathbf{u}}(N-1) \\ \vdots & \vdots & \ddots & \vdots \\ \underline{\mathbf{u}}(i-1) & \underline{\mathbf{u}}(i) & \cdots & \underline{\mathbf{u}}(i+N-2) \end{bmatrix},$$

where the subscripts, "$0''$ and "$i-1''$, indicate the time stamps of the $(1,1)$ and $(i,1)$ block elements of the matrix, respectively, and $N \to \infty$. Accordingly, we extend Eqn. 7 to

$$\underline{\mathbf{Y}}_{0,i-1} = \underline{\mathbf{\Gamma}}_i \mathbf{X}_0 + \underline{\mathbf{H}}_i \underline{\mathbf{U}}_{0,i-1} + \underline{\mathbf{\Pi}}_{0,i-1} \tag{8}$$

where, $\underline{\mathbf{Y}}_{0,i-1}$ and $\underline{\mathbf{\Pi}}_{0,i-1}$ are block Hankel matrices of $\{\underline{\mathbf{y}}_i(k)\}$ and $\{\underline{\boldsymbol{\pi}}_i(k)\}$, respectively; $\mathbf{X}_0 = [\mathbf{x}(0)\ \mathbf{x}(1)\ \cdots\ \mathbf{x}(N-1)]$, in which the subscript "$0''$ stands for the time instant of the first vector $\mathbf{x}(0)$. It follows from Eqn. 8 that

$$\mathbf{X}_0 = \underline{\mathbf{\Gamma}}_i^{+} \left(\underline{\mathbf{Y}}_{0,i-1} - \underline{\mathbf{H}}_i \underline{\mathbf{U}}_{0,i-1} - \underline{\mathbf{\Pi}}_{0,i-1} \right) \tag{9}$$

where $\underline{\mathbf{\Gamma}}_i^{+}$ is the Moore-Penrose pseudo inverse of $\underline{\mathbf{\Gamma}}_i$, and has a rank of n.

Eqn. 7 can also be extended to

$$\underline{\mathbf{Y}}_{i,2i-1} = \underline{\mathbf{\Gamma}}_i \mathbf{X}_i + \underline{\mathbf{H}}_i \underline{\mathbf{U}}_{i,2i-1} + \underline{\mathbf{\Pi}}_{i,2i-1} \tag{10}$$

where $\underline{\mathbf{Y}}_{i,2i-1}$, $\underline{\mathbf{\Pi}}_{i,2i-1}$, and $\underline{\mathbf{U}}_{i,2i-1}$ are analogous to $\underline{\mathbf{Y}}_{0,i}$, $\underline{\mathbf{\Pi}}_{0,i}$ and $\underline{\mathbf{U}}_{0,i}$, respectively;

$$\mathbf{X}_i = \underline{\mathbf{A}}^i \mathbf{X}_0 + \underline{\Delta}_i \underline{\mathbf{U}}_{0,i-1} + \underline{\Delta}_i^s \underline{\mathbf{\Omega}}_{0,i-1} \tag{11}$$

is derived from Eqn. 6; $\underline{\mathbf{\Omega}}_{0,i-1}$ is the block Hankel matrix of $\underline{\boldsymbol{\omega}}_i(k)$. Eqns. 9, 10, and 11 are the Hankel matrix-based stacked equations. Their combination readily shows that $\underline{\mathbf{Y}}_{i,2i-1}$ is a linear combination of $\underline{\mathbf{U}}_{0,i}$, $\underline{\mathbf{Y}}_{0,i}$, and $\underline{\mathbf{U}}_{i,2i-1}$.

B. Identification Algorithms

For two compatible matrices, $\mathbf{A}_1$ and $\mathbf{A}_2$, we denote

$$\mathbf{A}_1/\mathbf{A}_2 \equiv \mathbf{A}_1 \mathbf{A}_2' \left(\mathbf{A}_1 \mathbf{A}_2'\right)^{-1} \mathbf{A}_2 \tag{12}$$

as the projection of $\mathbf{A}_1$ onto the row space of $\mathbf{A}_2$. $\mathbf{A}_1/\mathbf{A}_2$ is the optimal prediction of $\mathbf{A}_1$ based on $\mathbf{A}_2$ in the sense that the squared F-norm, $\|\mathbf{A}_1 - \mathbf{A}_2\|_F^2$, is minimized subject to: row space of $\mathbf{A}_1 \subset$ row space of $\mathbf{A}_2$.

We summarize the identification algorithms as follows.

- Using Eqn. 12, calculate

$$\begin{aligned} \underline{\mathbf{Z}}_i &= \underline{\mathbf{Y}}_{i,2i-1} / \begin{bmatrix} \underline{\mathbf{U}}_{0,2i-1} \\ \underline{\mathbf{Y}}_{0,i-1} \end{bmatrix} \\ &= \begin{bmatrix} \mathbf{L}_i^1 | & \mathbf{L}_i^2 | & \mathbf{L}_i^3 \end{bmatrix} \begin{bmatrix} \underline{\mathbf{U}}_{0,i-1} \\ \underline{\mathbf{U}}_{i,2i-1} \\ \underline{\mathbf{Y}}_{0,i-1} \end{bmatrix} \text{ and} \end{aligned}$$

$$\begin{aligned} \underline{\mathbf{Z}}_{i+1} &= \underline{\mathbf{Y}}_{i+1,2i-1} / \begin{bmatrix} \underline{\mathbf{U}}_{0,2i-1} \\ \underline{\mathbf{Y}}_{0,i} \end{bmatrix} \\ &= \begin{bmatrix} \mathbf{L}_{i+1}^1 | & \mathbf{L}_{i+1}^2 | & \mathbf{L}_{i+1}^3 \end{bmatrix} \begin{bmatrix} \underline{\mathbf{U}}_{0,i-1} \\ \underline{\mathbf{U}}_{i,2i-1} \\ \underline{\mathbf{Y}}_{0,i} \end{bmatrix}. \end{aligned}$$

- Calculate the singular value decomposition:

$$\begin{bmatrix} \mathbf{L}_i^1 | & \mathbf{L}_i^3 \end{bmatrix} \begin{bmatrix} \underline{\mathbf{U}}_{0,i-1} \\ \underline{\mathbf{Y}}_{0,i-1} \end{bmatrix} = \mathbf{U}_1 \mathbf{\Lambda}_1 \mathbf{V}_1',$$

where $\mathbf{\Lambda}_1$ is a diagonal matrix containing the non-zero singular values, and $\mathbf{U}_1$ and $\mathbf{V}_1$ are the associated left and right singular vectors, respectively. Select $\underline{\mathbf{\Gamma}}_i = \mathbf{U}_1 \mathbf{\Lambda}_1^{1/2}$.

- Determining the least squares solution:

$$\begin{aligned} \begin{bmatrix} \underline{\mathbf{\Gamma}}_{i-1}^{+} \underline{\mathbf{Z}}_{i+1} \\ \underline{\mathbf{Y}}_{i,i} \end{bmatrix} &= \begin{bmatrix} \mathbf{K}_{11} & \mathbf{K}_{12} \\ \mathbf{K}_{21} & \mathbf{K}_{22} \end{bmatrix} \begin{bmatrix} \underline{\mathbf{\Gamma}}_i^{+} \underline{\mathbf{Z}}_i \\ \underline{\mathbf{U}}_{i,2i-1} \end{bmatrix} \\ &+ \underline{\mathbf{\Psi}}_i, \end{aligned}$$

results in $\underline{\mathbf{A}} \leftarrow \mathbf{K}_{11}$, $\underline{\mathbf{C}} \leftarrow \mathbf{K}_{21}$, $\mathbf{K}_{12} = [\mathbf{K}_{12}^1\ |\mathbf{K}_{12}^2]$, and $\mathbf{K}_{22} = [\mathbf{K}_{22}^1\ |\mathbf{K}_{22}^2]$, where $\underline{\mathbf{\Psi}}_i$ is the error matrix. Note that

$$\mathbf{K}_{12}^2 = \underline{\mathbf{\Gamma}}_{i-1}^{+} \underline{\mathbf{H}}_{i-1} - \underline{\mathbf{A}}\ \underline{\mathbf{\Gamma}}_i^{+} \begin{bmatrix} \mathbf{0} \\ \underline{\mathbf{H}}_{i-1} \end{bmatrix} \text{ and}$$

$$\mathbf{K}_{22}^2 = -\underline{\mathbf{C}}\ \underline{\mathbf{\Gamma}}_i^{+} \begin{bmatrix} \mathbf{0} \\ \underline{\mathbf{H}}_{i-1} \end{bmatrix}$$

can give solution to $\underline{\mathbf{H}}_{i-1}$. Furthermore, from

$$\mathbf{K}_{22}^1 = \underline{\mathbf{D}} - \underline{\mathbf{C}}\ \underline{\mathbf{\Gamma}}_i^{+} \begin{bmatrix} \underline{\mathbf{D}} \\ \underline{\mathbf{\Gamma}}_{i-1} \underline{\mathbf{B}} \end{bmatrix} \text{ and}$$

$$\mathbf{K}_{12}^1 = \underline{\mathbf{B}} - \underline{\mathbf{A}}\ \underline{\mathbf{\Gamma}}_i^{+} \begin{bmatrix} \underline{\mathbf{D}} \\ \underline{\mathbf{\Gamma}}_{i-1} \underline{\mathbf{B}} \end{bmatrix},$$

$\underline{\mathbf{B}}$ and $\underline{\mathbf{D}}$ can be calculated.

- From $\underline{\mathbf{\Psi}}_i$, calculate the covariance matrices,

$$\begin{bmatrix} \underline{\mathbf{R}}_{\omega} & \underline{\mathbf{R}}_{\omega,\varepsilon}' \\ \underline{\mathbf{R}}_{\omega,\varepsilon} & \underline{\mathbf{R}}_{\varepsilon} \end{bmatrix} = \frac{1}{N} \underline{\mathbf{\Psi}}_i \underline{\mathbf{\Psi}}_i'.$$

IV. KALMAN FILTER-BASED FDI IN NUSM SYSTEMS

Kalman filters have extensive applicability. Especially, since the pioneering work of Mehra and Peschon [16], they have been frequently applied to FDI in single rate systems. A survey of this area has been provided by Frank [17] and the most recent work has been reported by Keller [18].

Recently research attention has focused on FDI of uniformly sampled multirate systems [19], [20]. FDI in NUSM systems has also been considered [21] by extending the Chow-Willsky scheme [22]. In addition, the use of Kalman filters for sensor fault detection in NUSM systems [6] has been investigated. This paper proposes a novel Kalman filter-based approach towards sensor and actuator FDI in NUSM systems.

A. Fault detection in NUSM systems

Typically, a plant with actuator and sensor faults can be depicted by Fig. 1. In the plant, the measured outputs with sensor faults, for $j = [1, n_i]$, can be represented by

$$\mathbf{y}(kT + t_i^j) = \mathbf{y}^*(kT + t_i^j) + \mathbf{f}_y(kT + t_i^j) \tag{13}$$

where $\mathbf{y}^*(kT + t_i^j) = \tilde{\mathbf{y}}(kT + t_i^j) + \mathbf{o}(kT + t_i^j)$ is the fault-free value, and $\mathbf{f}_y(kT + t_i^j)$ is the fault magnitude vector

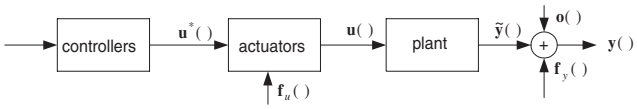

Fig. 1. Schematic diagram of a system with actuator and sensor faults

with zero and non-zero elements. For instance, if the first and third sensors are faulty, the first and third elements in $\mathbf{f}_y(kT+t_i^j)$ are non-zero, while other elements are zero.

The inputs to a plant, or the outputs of actuators, can be similarly represented by

$$\mathbf{u}(kT+t_i) = \mathbf{u}^*(kT+t_i) + \mathbf{f}_u(kT+t_i) \tag{14}$$

where $\mathbf{u}^*(kT+t_i)$ are the fault-free values; $\mathbf{f}_u(kT+t_i)$ is the fault vector in the actuators and analogous to $\mathbf{f}_y(\ )$ in structure. Note that $\mathbf{u}^*(kT+t_i)$ are available, because they are outputs of controllers. However, $\mathbf{u}(kT+t_i)$ are not available. Given data: $\{\mathbf{u}^*(kT+t_i)\}$ and $\{\mathbf{y}(kT+t_i^j)\}$, for $i=[1,g]$, $j=[1,n_i]$, and $k=[1,2,\cdots)$, the purpose of fault detection is to indicate when any elements in $\mathbf{f}_u(\ )$ and/or $\mathbf{f}_y(\ )$ begin to be non-zero. We define two lifted vectors:

$$\begin{aligned} \underline{\mathbf{u}}(k) &= \underline{\mathbf{u}}^*(k) + \underline{\mathbf{f}}_u(k) \\ \underline{\mathbf{y}}(k) &= \underline{\mathbf{y}}^*(k) + \underline{\mathbf{f}}_y(k) \end{aligned}$$

where $\underline{\mathbf{f}}_y(k)$ is structurally similar to $\underline{\mathbf{y}}(k)$ ($\underline{\mathbf{y}}^*(k)$), and so is $\underline{\mathbf{f}}_u(k)$ to $\underline{\mathbf{u}}(k)$ ($\underline{\mathbf{u}}^*(k)$). Accordingly, we rewrite Eqn. 4 as

$$\begin{aligned} \mathbf{x}(k+1) &= \underline{\mathbf{A}}\ \mathbf{x}(k) + \underline{\mathbf{B}}\ \underline{\mathbf{u}}^*(k) + \underline{\mathbf{B}}\ \underline{\mathbf{f}}_u(k) + \underline{\boldsymbol{\omega}}(k) \\ \underline{\mathbf{y}}(k) &= \underline{\mathbf{C}}\ \mathbf{x}(k) + \underline{\mathbf{D}}\ \underline{\mathbf{u}}^*(k) + \underline{\mathbf{D}}\ \underline{\mathbf{f}}_u(k) + \underline{\mathbf{f}}_y(k) + \\ &\quad \underline{\boldsymbol{\varepsilon}}(k) \end{aligned} \tag{15}$$

The substitution of $\underline{\mathbf{y}}(k)$ in Eqn. 15 into Eqn. 5 gives

$$\begin{aligned} \hat{\mathbf{x}}(k+1|k) &= \underline{\mathbf{A}}\ \hat{\mathbf{x}}(k|k-1) + \underline{\mathbf{B}}\ \underline{\mathbf{u}}^*(k) + \\ &\quad \underline{\mathbf{L}}\bar{\mathbf{y}}(k|k-1) \end{aligned} \tag{16}$$

where

$$\begin{aligned} \bar{\underline{\mathbf{y}}}(k|k-1) &\equiv \underline{\mathbf{y}}(k) - \hat{\underline{\mathbf{y}}}(k|k-1) \\ &= \underline{\mathbf{C}}\bar{\mathbf{x}}(k|k-1) + \underline{\mathbf{D}}\ \underline{\mathbf{f}}_u(k) + \underline{\mathbf{f}}_y(k) \\ &\quad + \ \underline{\boldsymbol{\varepsilon}}(k) \end{aligned} \tag{17}$$

with $\underline{\mathbf{L}}$ being a steady value of $\underline{\mathbf{L}}(k)$; $\bar{\mathbf{x}}(i|i-1) = \mathbf{x}(i) - \hat{\mathbf{x}}(i|i-1)$ is the state estimation error for $i=k$ or $i=k+1$. Furthermore, subtracting $\mathbf{x}(k+1)$ in Eqn. 15 using Eqn. 16 leads to

$$\begin{aligned} \bar{\mathbf{x}}(k+1|k) &= (\underline{\mathbf{A}} - \underline{\mathbf{L}}\ \underline{\mathbf{C}})\ \bar{\mathbf{x}}(k|k-1) - \underline{\mathbf{L}}\ \underline{\mathbf{f}}_y(k) + \\ &\quad (\underline{\mathbf{B}} - \underline{\mathbf{L}}\ \underline{\mathbf{D}})\,\underline{\mathbf{f}}_u(k) + \underline{\boldsymbol{\omega}}(k) - \underline{\mathbf{L}}\ \underline{\boldsymbol{\varepsilon}}(k). \end{aligned}$$

From the preceding equation it can be shown that

$$\begin{aligned} \bar{\mathbf{x}}(k|k-1) &= \sum_{i=0}^{k-1} (\underline{\mathbf{A}} - \underline{\mathbf{L}}\ \underline{\mathbf{C}})^{k-1-i} \bullet \\ &\quad [(\underline{\mathbf{B}} - \underline{\mathbf{L}}\ \underline{\mathbf{D}})\underline{\mathbf{f}}_u(i) - \underline{\mathbf{L}}\ \underline{\mathbf{f}}_y(i)] \\ &\quad + \ \bar{\mathbf{x}}^*(k|k-1) \end{aligned} \tag{18}$$

where,

$$\begin{aligned} \bar{\mathbf{x}}^*(k|k-1) &= (\underline{\mathbf{A}} - \underline{\mathbf{L}}\ \underline{\mathbf{C}})^k\, \bar{\mathbf{x}}(0|-1) + \\ &\quad \sum_{i=0}^{k-1} (\underline{\mathbf{A}} - \underline{\mathbf{L}}\ \underline{\mathbf{C}})^{k-1-i}\, [\underline{\boldsymbol{\omega}}(i) - \underline{\mathbf{L}}\ \underline{\boldsymbol{\varepsilon}}(i)\ ]. \end{aligned}$$

Finally, the substitution of Eqn. 18 into Eqn. 17 produces

$$\bar{\underline{\mathbf{y}}}(k|k-1) = \bar{\underline{\mathbf{y}}}^*(k|k-1) + \bar{\underline{\mathbf{y}}}^f(k|k-1) \tag{19}$$

where

$$\begin{aligned} \bar{\underline{\mathbf{y}}}^*(k|k-1) &= \underline{\mathbf{C}} \sum_{i=0}^{k-1} (\underline{\mathbf{A}} - \underline{\mathbf{L}}\ \underline{\mathbf{C}})^{k-1-i}\, [\underline{\boldsymbol{\omega}}(i) - \underline{\mathbf{L}}\ \underline{\boldsymbol{\varepsilon}}(i)\ ] \\ &\quad + \ \underline{\mathbf{C}}\,(\underline{\mathbf{A}} - \underline{\mathbf{L}}\ \underline{\mathbf{C}})^k\, \bar{\mathbf{x}}(0|-1) \sim \aleph\,[\mathbf{0}, \underline{\mathbf{G}}(k)] \end{aligned}$$

as proved in [6];

$$\begin{aligned} \bar{\underline{\mathbf{y}}}^f(k|k-1) &= \underline{\mathbf{C}} \sum_{i=0}^{k-1} (\underline{\mathbf{A}} - \underline{\mathbf{L}}\ \underline{\mathbf{C}})^{k-1-i} \bullet \\ &\quad [(\underline{\mathbf{B}} - \underline{\mathbf{L}}\ \underline{\mathbf{D}})\underline{\mathbf{f}}_u(i) - \underline{\mathbf{L}}\ \underline{\mathbf{f}}_y(i)] \\ &\quad + \ \underline{\mathbf{D}}\ \underline{\mathbf{f}}_u(k) + \underline{\mathbf{f}}_y(k). \end{aligned}$$

In accordance with [23], it can be shown that $\underline{\mathbf{A}} - \underline{\mathbf{L}}\ \underline{\mathbf{C}}$ has stable eigenvalues. Perform an eigendecomposition (ED) on $\underline{\mathbf{A}} - \underline{\mathbf{L}}\ \underline{\mathbf{C}}$, e.g., $\underline{\mathbf{A}} - \underline{\mathbf{L}}\ \underline{\mathbf{C}} = \underline{\mathbf{U}}_A \underline{\boldsymbol{\Lambda}}_A \underline{\mathbf{U}}_A^{-1}$, where $\underline{\boldsymbol{\Lambda}}_A$ is a diagonal matrix containing $n_\circ$ ($\leq n$) non-zero eigenvalues and $\underline{\mathbf{U}}_A$ are the associated eigenvectors. Using this ED in Eqn. 19 leads to

$$\begin{aligned} \bar{\underline{\mathbf{y}}}^f(k|k-1) &= \underline{\mathbf{D}}\ \underline{\mathbf{f}}_u(k) + \underline{\mathbf{f}}_y(k) + \underline{\mathbf{C}}\ \underline{\mathbf{U}}_A \sum_{i=0}^{k-1} \underline{\boldsymbol{\Lambda}}_A^{k-1-i} \\ &\quad \bullet \underline{\mathbf{U}}_A^{-1} [(\underline{\mathbf{B}} - \underline{\mathbf{L}}\ \underline{\mathbf{D}})\underline{\mathbf{f}}_u(i) - \underline{\mathbf{L}}\ \underline{\mathbf{f}}_y(i)], \end{aligned}$$

where $\underline{\mathbf{C}}\ \underline{\mathbf{U}}_A$ is $mp \times n_\circ$-dimensional, and mp is usually much larger than $n_\circ$.

For $\underline{\mathbf{C}}\ \underline{\mathbf{U}}_A$, if its rank is n_1 ($\leq n_\circ$), then the rank of its null space is $mp - n_1$. Selecting a matrix, $\underline{\mathbf{W}}_\circ$, from such a null space, i.e. $\underline{\mathbf{W}}_\circ \underline{\mathbf{C}}\ \underline{\mathbf{U}}_A \equiv \mathbf{0}$, we define

$$\begin{aligned} \underline{\mathbf{e}}(k) &\equiv \underline{\mathbf{W}}_\circ \bar{\underline{\mathbf{y}}}(k|k-1) \\ &= \underline{\mathbf{e}}^*(k) + \underline{\mathbf{e}}^f(k) \in \Re^{mp-n_\circ} \end{aligned} \tag{20}$$

as the primary residual vector (PRV) for fault detection. In Eqn. 20, $\underline{\mathbf{e}}^*(k) = \underline{\mathbf{W}}_\circ \bar{\underline{\mathbf{y}}}^*(k|k-1)$ is the fault-free component, while

$$\underline{\mathbf{e}}^f(k) = \underline{\mathbf{W}}_\circ \bar{\underline{\mathbf{y}}}^f(k|k-1) = [\underline{\mathbf{W}}_\circ \underline{\mathbf{D}} \mid \underline{\mathbf{W}}_\circ] \begin{bmatrix} \underline{\mathbf{f}}_u(k) \\ \underline{\mathbf{f}}_y(k) \end{bmatrix}$$

is the fault-contribution component.

Besides satisfying $\underline{\mathbf{W}}_\circ \underline{\mathbf{C}}\ \underline{\mathbf{U}}_A = \mathbf{0}$, $\underline{\mathbf{W}}_\circ$ should also have maximized covariance with $\underline{\mathbf{D}}$ such that the PRV will have maximized sensitivity to any faults. In line with [24] and [25],

$$\begin{aligned} \underline{\mathbf{W}}'_\circ &= \text{the singular vectors corresponding} \\ &\quad \text{to } mp - n_1 \text{ non-zero singular values of} \\ &\quad [\mathbf{I}_{mp} - \underline{\mathbf{C}}\ \underline{\mathbf{U}}_A\,(\underline{\mathbf{C}}\ \underline{\mathbf{U}}_A)^+]\underline{\mathbf{D}} \end{aligned} \tag{21}$$

It can be shown that $\underline{\mathbf{e}}(k) = \underline{\mathbf{e}}^*(k) \sim \aleph[\mathbf{0}, \underline{\mathbf{R}}_e(k)]$ in the absence of fault, or $\underline{\mathbf{e}}(k) \sim \aleph\left[\underline{\mathbf{e}}^f(k), \underline{\mathbf{R}}_e(k)\right]$ in the presence of any faults, where $\underline{\mathbf{R}}_e(k) = \underline{\mathbf{W}}_\circ \underline{\mathbf{G}}(k) \underline{\mathbf{W}}'_\circ$. Therefore, fault detection can be conducted by testing the whiteness of the PRV. Define a scalar $f_D(k) = \underline{\mathbf{e}}'(k)\underline{\mathbf{R}}_e^{-1}(k)\underline{\mathbf{e}}(k)$, which follows a (non-central) chi-square distribution with $mp - n_1$ degrees of freedom in the normal (faulty) case [26]. Given a threshold, $\chi^2_\beta(mp - n_1)$, for $f_D(k)$, where β is a level of significance. While $f_D(k) < \chi^2_\beta(mp - n_1)$ indicates the absence of fault, $f_D(k) \geq \chi^2_\beta(mp - n_1)$ triggers fault alarms.

B. Fault isolation

To isolate each faulty actuator/sensor, one needs to transform the PRV into a set of structured residual vectors (SRVs). For simplicity, assume that at each time, only a single actuator/sensor is faulty in this paper. For isolation of multiple faulty sensors/actuators, interested readers are referred to [27] for details.

There are l actuators and m sensors in the considered system. Accordingly $(l + m)$ SRVs are designed. And each SRV is made insensitive to one specific faulty actuator/sensor but has maximized sensitivity to others. We call a sensor or an actuator an instrument for convenience. More specifically, the i^{th} SRV, $\underline{\mathbf{r}}_i(k)$, is designed to be insensitive to a fault in the i^{th} instrument, but most sensitive to faults in other instruments, for $i \in [1, l + m]$. The sensitivity and insensitivity of the $l + m$ SRVs with respect to the faulty instruments, also termed as *fault isolation logic*, are summarized in Table I. In the table, a "0"/"1" means the insensitivity/maximized sensitivity of a SRV to a faulty instrument. In addition, $f^i_u(\,)$/$f^j_y(\,)$ stands for the fault in the i^{th} actuator/j^{th} sensor, for $i \in [1, l]$/$j \in [1, m]$.

	$f^1_u(\,)$	$\cdots$	$f^l_u(\,)$	$f^1_y(\,)$	$\cdots$	$f^m_y(\,)$
$\underline{\mathbf{r}}_1(k)$	0	1	1	1	1	1
$\vdots$	$\vdots$	$\ddots$	$\vdots$	$\vdots$	$\ddots$	$\vdots$
$\underline{\mathbf{r}}_l(k)$	1	1	0	1	1	1
$\underline{\mathbf{r}}_{l+1}(k)$	1	1	1	0	1	1
$\vdots$	$\vdots$	$\ddots$	$\vdots$	$\vdots$	$\ddots$	$\vdots$
$\underline{\mathbf{r}}_{l+m}(k)$	1	$\cdots$	1	1	1	0

TABLE I

Sensitivity and insensitivity of the $l + m$ SRVs w.r.t. faulty actuators/sensors

Mathematically, the i^{th} SRV is

$$\underline{\mathbf{r}}_i(k) = \underline{\mathbf{W}}_i \underline{\mathbf{e}}(k) = \underline{\mathbf{r}}^*_i(k) + \underline{\mathbf{r}}^f_i(k),$$

where $\underline{\mathbf{r}}^*_i(k) = \underline{\mathbf{W}}_i \underline{\mathbf{e}}^*(k) \sim \aleph(\mathbf{0}, \underline{\mathbf{R}}_{e,i})$ with $\underline{\mathbf{R}}_{e,i} = \underline{\mathbf{W}}_i \underline{\mathbf{R}}_e \underline{\mathbf{W}}'_i$, and

$$\underline{\mathbf{r}}^f_i(k) = \underline{\mathbf{W}}_i \underline{\mathbf{e}}^f(k) = \underline{\mathbf{W}}_i [\underline{\mathbf{W}}_\circ \underline{\mathbf{D}} \mid \underline{\mathbf{W}}_\circ] \begin{bmatrix} \underline{\mathbf{f}}_u(k) \\ \underline{\mathbf{f}}_y(k) \end{bmatrix}.$$

Denote $\underline{\mathbf{\Theta}}_\circ \equiv [\underline{\mathbf{W}}_\circ \underline{\mathbf{D}} \mid \underline{\mathbf{W}}_\circ] \in \Re^{(mp-n_1)\times(mp+lg)}$. As a consequence, the fault model for the i^{th} SRV is $\underline{\mathbf{W}}_i \underline{\mathbf{\Theta}}_\circ$. Moreover, we can split $\underline{\mathbf{\Theta}}_\circ$ into two parts, e.g. $\underline{\mathbf{\Theta}}_\circ = [\underline{\mathbf{\Theta}}_{\circ,i} | \ \underline{\mathbf{\Theta}}^\perp_{\circ,i}]$, where $\underline{\mathbf{\Theta}}_{\circ,i}$ denotes those columns associated with fault in the i^{th} instrument, and $\underline{\mathbf{\Theta}}^\perp_{\circ,i}$ the remaining columns.

In the presence of a single sensor fault, ($\underline{\mathbf{f}}_u(k)$ is zero), from its definition $\underline{\mathbf{f}}_y(k)$ has p non-zero elements. As a consequence, $\underline{\mathbf{\Theta}}_{\circ,i}$ has p columns. Similarly, when a single actuator occurs ($\underline{\mathbf{f}}_y(k) = \mathbf{0}$), $\underline{\mathbf{f}}_u(k)$ has g non-zero elements, and hence $\underline{\mathbf{\Theta}}_{\circ,i}$ has g columns.

Since the i^{th} SRV is designed to be insensitive to any fault in the i^{th} instrument, it is required that $\underline{\mathbf{W}}_i$ is orthogonal to $\underline{\mathbf{\Theta}}_{\circ,i}$ but has maximized covariance with $\underline{\mathbf{\Theta}}^\perp_{\circ,i}$. Using the similar algorithms to calculate $\underline{\mathbf{W}}_\circ$, we can obtain $l + m$ transformation matrices,

$$\begin{aligned} \underline{\mathbf{W}}'_i \ = \ & \text{the singular vectors corresponding} \\ & \text{to non-zero singular values of} \\ & [\mathbf{I}_{mp-n_\circ} - \underline{\mathbf{\Theta}}_{\circ,i} \left(\underline{\mathbf{\Theta}}_{\circ,i}\right)^+] \underline{\mathbf{\Theta}}^\perp_{\circ,i}, \end{aligned} \tag{22}$$

$\forall\ i \in [1, l + m]$. Note that $\underline{\mathbf{W}}_i$ is $(mp - n_1 - g) \times (mp - n_1)$/$(mp - n_1 - p) \times (mp - n_1)$-dimensional when $\underline{\mathbf{\Theta}}^i_\circ$ has g/p columns.

After fault detection, it follows from the pre-determined isolation logic that

$$\underline{\mathbf{r}}_i(k) \sim \begin{cases} \aleph(\mathbf{0}, \underline{\mathbf{R}}_{e,i}), & \text{if the } i^{th} \text{ instrument fails;} \\ \aleph(\underline{\mathbf{r}}^f_i(k), \underline{\mathbf{R}}_{e,i}), & \text{if any other instrument fails;} \end{cases}$$

where $\underline{\mathbf{R}}_{e,i} = \underline{\mathbf{W}}_i \underline{\mathbf{R}}_e \underline{\mathbf{W}}'_i$. Define a scalar fault isolation index $\mathrm{f}_{I,i}(k) = \underline{\mathbf{r}}_i(k) \underline{\mathbf{R}}^{-1}_{e,i} \underline{\mathbf{r}}_i(k)$. If $\mathrm{f}_{I,i}(k)$ follows a chi-square distribution with degrees of freedom, $(mp - n_1 - g)/(mp - n_1 - p)$, then the i^{th} instrument is faulty. Otherwise, any other but the i^{th} instrument is faulty.

C. Analysis on fault detectability and isolability

The conditions under which a single fault is detectable and isolable will be analyzed in this subsection. In the PRV, note that

$$\underline{\mathbf{e}}^f(k) = [\underline{\mathbf{W}}_\circ \underline{\mathbf{D}} \mid \underline{\mathbf{W}}_\circ] \begin{bmatrix} \underline{\mathbf{f}}_u(k) \\ \underline{\mathbf{f}}_y(k) \end{bmatrix},$$

where the gain matrix for $\underline{\mathbf{f}}_u(k)$ is $\underline{\mathbf{W}}_\circ \underline{\mathbf{D}}$ and that for $\underline{\mathbf{f}}_y(k)$ is $\underline{\mathbf{W}}_\circ$. The detectability of a fault is ensured if $\underline{\mathbf{e}}^f(k)$ is always non-zero.

1) Fault detectability conditions: In the presence of a single actuator fault, $\underline{\mathbf{e}}^f(k) = \underline{\mathbf{W}}_\circ \underline{\mathbf{D}}\ \underline{\mathbf{f}}_u(k)$. Since $\underline{\mathbf{f}}_u(k)$ has g non-zero elements, $\underline{\mathbf{e}}^f(k)$ is a linear combination of g columns of $\underline{\mathbf{W}}_\circ \underline{\mathbf{D}}$ specified by the non-zero elements. Apparently, $\underline{\mathbf{e}}^f(k) \neq \mathbf{0}$ requires that any g columns in $\underline{\mathbf{W}}_\circ \underline{\mathbf{D}}$ are linearly independent.

In the presence of a single sensor fault, $\underline{\mathbf{e}}^f(k) = \underline{\mathbf{W}}_\circ \underline{\mathbf{f}}_y(k)$. It can be similarly understood that fault detectability is guaranteed if any p columns in $\underline{\mathbf{W}}_\circ$ are linearly independent.

2) Fault isolability conditions: To isolate the i^{th} actuator fault, except $\underline{\mathbf{r}}_i^f(k) = \underline{\mathbf{W}}_i\underline{\mathbf{W}}_\circ\underline{\mathbf{D}}\ \underline{\mathbf{f}}_u(k) = \mathbf{0}$, for any $j \in [1, l]$ and $j \neq i$, $\underline{\mathbf{r}}_j^f(k) = \underline{\mathbf{W}}_j\underline{\mathbf{W}}_\circ\underline{\mathbf{D}}\ \underline{\mathbf{f}}_u(k) \neq \mathbf{0}$ should be guaranteed. This requires that any g columns in $\underline{\mathbf{W}}_j\underline{\mathbf{W}}_\circ\underline{\mathbf{D}}$ are linearly independent. It can be similarly concluded that to isolate a single sensor fault, any p columns in $\underline{\mathbf{W}}_j\underline{\mathbf{W}}_\circ$ must be linearly independent.

V. An Experimental Case Study

In this section, an experimental case study is conducted to test the correctness of the proposed SMI algorithm and the utility of the FDI scheme.

A. The Experimental Pilot Plant

The experimental pilot plant is a continuous stirred tank heater system (CSTHS) located in the Computer Process Control Laboratory, at the University of Alberta. As shown in Fig. 2, the CSTHS has two inputs, i.e. $l = 2$, the cold and hot water flowrates, and two outputs, i.e. $m = 2$, the level and temperature of the water in the tank. The inputs are manipulated by respective controllers, and the outputs from the controllers drive the actuators, which are two valves. The ultimate purpose of the CSTHS is to regulate the outputs.

Fig. 2. Physical layout of the CSTHS system with the associated hardware

B. Identification of the lifted model of the pilot plant

Select a frame period, $T = 6$ secs. From this pilot plant, a set of training data covering 799 frame periods is collected to identify the lifted model. Within each frame period $[kT, kT + T]$ for $k = 0, 1, 2, \cdots$, the two inputs are sampled at instants kT, $kT + 3$, and $kT + 4$, while the two outputs are sampled at instants kT, $kT + 2$, and $kT + 5$. Thus, the lifted input and output vectors are

$$\underline{\mathbf{u}}(k) = \begin{bmatrix} \mathbf{u}(kT) \\ \mathbf{u}(kT+3) \\ \mathbf{u}(kT+4) \end{bmatrix},\ \underline{\mathbf{y}}(k) = \begin{bmatrix} \mathbf{y}(kT) \\ \mathbf{y}(kT+2) \\ \mathbf{y}(kT+5) \end{bmatrix},$$

where $g = p = 3$. From $\{\underline{\mathbf{u}}(k), \underline{\mathbf{y}}(k)\}$ for $k = 1, 2, \cdots, 799$, we construct three data matrices, $\underline{\mathbf{U}}_{0,i-1}$, $\underline{\mathbf{Y}}_{0,i-1}$, and $\underline{\mathbf{Y}}_{i,2i-1}$ with $i = 3$, and each matrix has 799 columns. Subsequently, applying the subspace identification algorithms developed in Section 3, we estimate the lifted model, $\mathbf{A}$, $\underline{\mathbf{B}}$, $\underline{\mathbf{C}}$, and $\underline{\mathbf{D}}$, and the noise covariances, $\underline{\mathbf{R}}_\epsilon$, $\underline{\mathbf{R}}_\omega$, and $\underline{\mathbf{R}}_{\omega,\varepsilon}$.

Using the identified matrices, we construct the Kalman filter, Eqn. 5. We also calculate $\underline{\mathbf{W}}_\circ$ and $\underline{\mathbf{W}}_i$ for $i \in [1, 4]$ in order to generate one PRV for fault detection and four SRVs for fault isolation. Note that we have employed the isolation logic in table I to design the SRVs, i.e. the i^{th} SRV is insensitive to fault in the i^{th} instrument, but has maximized sensitivity to faults in other instruments, for $i \in [1, 4]$. Finally, we calculate the covariances, $\underline{\mathbf{R}}_e$ and $\underline{\mathbf{R}}_{e,i}$ for the PRV and SRVs, for $i \in [1, 4]$.

1) Validation of the identified model: In addition to the data used for identification, another sequence of data covering 350 frame periods for the fault-free case was made available for model validation. From this data sequence, a sequence of PRVs, $\{\underline{\mathbf{e}}(k)\}$, is generated, where each PRV is 4-dimensional. Moreover, we calculate the fault detection index, $\mathrm{f}_D(k) = \underline{\mathbf{e}}'(k)\underline{\mathbf{R}}_e^{-1}\underline{\mathbf{e}}(k)$. In this fault-free case, $\mathrm{f}_D(k)$ follows a chi-square distribution with degrees of freedom equal to 4. Therefore, with a pre-selected level of significance $\beta = 0.01$, the confidence limit for $\mathrm{f}_D(k)$ is $\chi^2_{0.01}(4) = 13.277$. We scale $\mathrm{f}_D(k)$ by 13.277 and plot the scaled value, "FD", in Figure 3. Note that in the figure, each point in the x-axis represents a frame period, i.e. 6 seconds. As can be seen clearly, "FD" is within its confidence limit, 1, (with an acceptable rate of false alarm) indicating the validity of the identified model.

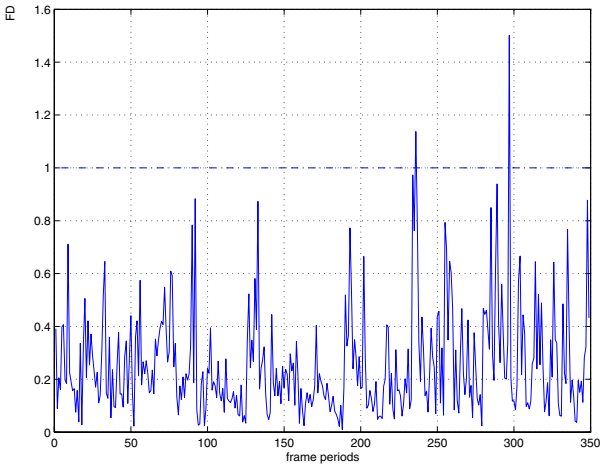

Fig. 3. The scaled fault detection index generated from the validation data

C. FDI results

Due to space limitation in this paper, FDI results for only one fault scenario are presented. However, we have carried out FDI in many other fault scenarios and interested readers are encouraged to contact the authors to obtain more details.

A random noise, $\aleph(0, 0.25^2)$, is introduced to an instrument at $t_f = 389 * 6 = 2334$ seconds. The test data are sampled at the same rate as the training data, and on-line and real-time FDI is carried out. The relevant FDI results

are depicted in Figure 4, where FD is the scaled fault detection index, and $\{FI_1, FI_2, FI_3, FI_4\}$ are the scaled fault isolation indices, respectively. It can be seen from the figure that FD is beyond the unit confidence limit after the occurrence of the fault. Therefore, fault detection has been successfully performed. Moreover, since FI_4 is unaffected by the fault, i.e. it is below the confidence limit (except at few statistically insignificant periods of time due to errors of chance, it is beyond the limits), while $\{FI_1, FI_2, FI_3\}$ are affected by the fault, i.e. they are beyond the confidence limit. The sensitivity of the 4 fault isolation indices can be characterized by a binary code $[1\ 1\ 1\ 0]$. Thus it can be inferred that the second sensor has a fault.

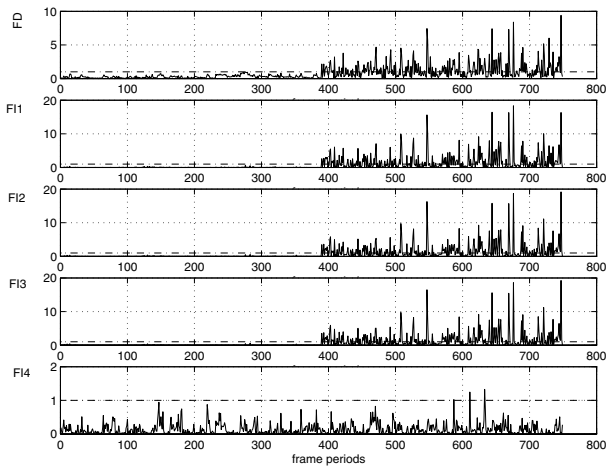

Fig. 4. Detection and isolation of a fault in the 2^{nd} sensor. The sensitivity of the isolation indices to the fault is $[1\ 1\ 1\ 0]$.

VI. Conclusion

Data-driven Kalman filters for NUSM systems have been proposed. A novel Kalman filter-based FDI methodology has been investigated. Analysis on fault detectability and isolability has been conducted. This developed FDI scheme has been applied to an experimental pilot plant, i.e. the CSTHS system in the Computer Process Control laboratory, at The University of Alberta. Different types of actuator and sensor faults in the CSTHS system, including drift and precision degradation, are successfully detected and isolated. Therefore, the practicality and utility of the proposed methodology have been demonstrated.

VII. Acknowledgements

Financial aid from the Natural Sciences and Engineering Research Council of Canada (NSERC), Matrikon Inc., and the Alberta Science Research Authority of Canada is gratefully acknowledged.

References

[1] R. Kalman, "A new approach to linear filtering and prediction problems," *Trans. ASME, J. Basic Eng.*, ser. 82D, pp 35-45, 1960.

[2] S. Haykin, *Adaptive Filter Theory*. 3th Edition, Prentice-Hall, New Jersey, 1996.

[3] H. Sorenson, "Least-squares estimation: from Gauss to Kalman," *IEEE Spectrum*, vol. 7, pp 63-68, 1970.

[4] H. Sorenson, *Kalman filtering: theory and application* (Ed.). IEEE Press, New York, 1985.

[5] R. Gudi, S.L. Shah and M. Gary, "Adaptive multirate state and parameter estimation strategies with application to a bioreactor," *AIChE J.*, vol. 41, pp. 2451-2464, 1994.

[6] W. Li and S.L. Shah, "Kalman Filters for non-uniformly sampled systems," to be presented at the *16th IFAC World Congress*, Prague, Czec Republic, 2005.

[7] M. Moonen, B. DeMoor, L. Vandenberghe and J. Vandewalle, "On and off-line identification of linear state-space models," *International Journal of Control*, vol. 49, 219–232, 1989.

[8] M. Verhaegen and P. Dewilde, "Subspace model identification. part i: the output-error state-space model identification class of algorithms," *International Journal of Control*, vol. 56, pp 1187-1210, 1992.

[9] M. Verhaegen and P. Dewilde, "Subspace model identification. part ii: Analysis of the elementary output-error state-space model identification algorithm," *International Journal of Control*, vol. 56, pp 1211-1241, 1992.

[10] L. Ljung, *System Identification: Theory for the User*. Prentice-Hall, New Jersey, 1987.

[11] P. Van Overschee and B. De Moor, "A unifying theorem for three subspace system identification algorithms," *Automatica*, vol. 31, pp 1853-1864, 1995.

[12] D. Li, S.L. Shah and T. Chen, "Identification of fast-rate models from multirate data," *International J. of Control*, vol. 74, pp 680-689, 2001.

[13] W. Li, Z. Han and S.L. Shah, "Subspace identification for FDI in systems with non-uniformly sampled multirate data," *Automatica*, accepted in Feburary, 2005.

[14] J. Sheng, T. Chen and S.L. Shah, "Generalized predictive control for non-uniformly sampled systems," *J. of Process Control*, vol. 12, pp 875-885, 2002.

[15] P. Van Overschee and B. De Moor, "N4SID: subspace algorithms for the identification of combined deterministic-stochastic systems," *Automatica*, vol. 30, pp 75-93, 1994.

[16] R. Mehra and I. Peschon, "An Innovations Approach to fault detection and diagnosis in dynamic systems," *Automatica*, vol. 7, pp 637-640, 1971.

[17] P. Frank, "Fault diagnosis in dynamic systems using analytical and knowledge-based redundancy – a survey and some new results," *Automatica*, vol. 26, pp. 459-474, 1990.

[18] J. Keller, "Fault isolation filter design for linear stochastic systems," *Automatica*, vol. 35, pp 1701-1706, 1999.

[19] M. Fadali and H. Emara-Shabaik, "Timely robust detection for multirate linear systems," *International J. of Control*, vol. 75, pp. 305-313, 2002.

[20] P. Zhang, S. Ding, G. Wang and D. Zhou, "Fault detection for multirate sample-data systems with time delay," *International J. of Control*, vol 75, pp 1457-1471, 2002.

[21] W. Li and S.L. Shah, "Fault detection and isolation in non-uniformly sampled systems," In: *Proc. of IFAC DYCOPS 7*, Cambridge, MA, 2004, 6p.

[22] E. Chow and A. Willsky, "Analytical redundancy and the design of robust failure detection systems," *IEEE Trans. Auto. Cont.*, vol. 29, pp. 603-614, 1984.

[23] C. Souza, M. Gevers and G. Goodwin (1986). Riccati equations in optimal filtering of nonstabilizable systems having singular state transition matrice. *IEEE Trans. Auto. Cont.*, vol. 30, pp. 831-838, 1986.

[24] G. Golub, "Some modified matrix eigenvalue problems," *SIAM Rev.*, vol. 15, pp. 318-334, 1973.

[25] C. Rao, "The use and interpretation of principal component analysis in applied research," *The Indian J. of Statistics, Series A*, vol. 26, pp 329-358, 1964.

[26] M. Basseville and I. Nikiforov, *Detection of Abrupt Changes–Theory and Applications*, Prentice-Hall, New Jersy, 1993.

[27] W. Li and S.L. Shah, "Strutured residual vector-based approach to sensor fault detection and isolation," *J. of Process Control*, vol. 12, pp 429-443, 2002.